ISSN 1063-7737, Astronomy Letters, 2013, Vol. 39, No. 7, pp. 474–480. © Pleiades Publishing, Inc., 2013.
Original Russian Text © N.A. Lotova, V.N. Obridko, 2013, published in Pis'ma v Astronomicheskiĭ Zhurnal, 2013, Vol. 39, No. 7, pp. 538–544.

Dependence of the Solar Wind Speed on the Coronal Magnetic Field in Cycle 23

N. A. Lotova* **and V. N. Obridko**

Pushkov Institute of Terrestrial Magnetism, Ionosphere, and Radio Wave Propagation (IZMIRAN), Russian Academy of Sciences, Troitsk, Moscow oblast, 142190 Russia

Received December 10, 2012

Abstract—The dependence of the position of the solar wind sonic point on the magnetic field in the solar corona during cycle 23 is studied. This dependence is shown to be rather strong in the rising phase and at the cycle maximum. As the coronal magnetic field grows, the distance to the sonic point decreases. Since the distance to the sonic point has been shown previously to anticorrelate with the solar wind speed, the result obtained suggests a strong positive correlation between the later and the coronal magnetic field. The situation changed dramatically two years after the calendar date of the cycle maximum. Beginning in 2004 the solar wind speed ceased to depend on the magnetic field up until the cycle minimum in December 2008. In 2009 a strong dependence of the wind speed on the coronal magnetic field was restored. It is hypothesized that this effect is associated with two different coronal heating mechanisms whose relative efficiency, in turn, depends on the contribution from magnetic fields of different scales.

DOI: 10.1134/S1063773713070049

Keywords: *solar magnetic field, solar wind, radio occultation method.*

NEW METHODS FOR STUDYING THE SOLAR WIND

In recent years, new possibilities for studying the solar wind have appeared. They allow the solar cycles to be studied using the solar wind, because the latter is an extension of the coronal magnetic fields into interplanetary space. A new, modern modification of the radio occultation method based on the simultaneous use of two previously known modifications of the method in studying the same region of the interplanetary medium has been developed to experimentally study the solar wind (Lotova et al. 2010, 2011). Such an approach was not used in previous studies (Kojima et al. 1998; Schwenn 2006).

The solar wind acceleration is not a single-stage process. Near the Sun, at distances $R \sim (10-30)R_\odot$, the solar wind flow is accelerated by sonic waves. As a result, the solar wind becomes supersonic. Subsequently, as one moves away into interplanetary space, the already supersonic flow is reaccelerated by magnetosonic waves at radial distances $R \sim (30-60)R_\odot$ and, further out at distances $R > 60R_\odot$, the solar wind is additionally accelerated by Alfvén waves. Since the main goal of this paper is to study the relationship between the supersonic flow and the coronal magnetic fields, we dwelt on the acceleration region nearest to the Sun, the transonic region of the solar wind.

In the new modification, the radio occultation method is used at radial distances $R \approx (2.5-70)R_\odot$ from the Sun, including the formation region of the supersonic solar wind. Two regimes, strong and weak radio wave scattering, are studied simultaneously (Lotova et al. 2010, 2011). In the first case, the observations were carried out on the DKR-1000 radio telescope at the Pushchino Radio Astronomy Observatory of the Russian Academy of Sciences at wavelength $\lambda \sim 3$ m, where quasars were used as occulted sources. In the regime of strong radio wave scattering, the radial dependence of the scattering angle $2\Theta(R)$ is studied. In the second case, the RT-22 radio telescope at wavelength $\lambda = 1.35$ cm is used and water vapor masers serve as occulted sources. In this case, the radial dependence of the scintillation index $m(R)$ is studied in the regime of weak scattering. An independent use of the two modifications of the radio occultation method simultaneously or at close dates allowed us to expand considerably the statistics of occulted sources approaching the Sun at small angular distances and, on this basis, to pass to large-scale radio-astronomical experiments on sounding the circumsolar interplanetary plasma. The experimental data allow the the boundaries of the transition, transonic region of the solar wind to be localized in interplanetary space : the

*E-mail: lotova@izmiran.ru

inner (R_{in}) and outer (R_{out}) boundaries. The inner boundary is of particular importance, because it is at this point that the solar wind speed begins to exceed the local speed of sound. Therefore, this point is often called the sonic point on one-dimensional diagrams. Radio maps of the heliolatitude structure of the solar wind can be constructed from these data.

In another new method, the restructuring of the radial magnetic fields in the upper solar corona on the source surface $R \sim 2.5R_\odot$ forming an inhomogeneous, jet structure of the solar wind flow is studied. This method is based on analysis of the correlation between the position of the solar wind sonic point $R_{in}(\varphi)$, where φ is the heliolatitude, on the magnetic field strength in the solar corona at a point conjugate to the position of the sonic point R_{in}:

$$R_{in} = F(|B_R|), \quad R = 2.5R_\odot. \qquad (1)$$

The correlation diagram for this dependence breaks up into discrete branches, the types of solar wind flows, which differ in different annual phases of the solar cycle (Lotova et al. 2010, 2011). In addition to the data from Kojima et al. (1999) and Schwenn (2006), we performed theoretical calculations of the magnetic fields in the solar corona (Obridko and Yermakov 1989; Obridko and Schelting 1992), which allowed eleven types of flows to be identified in solar cycle 23.

Of course, if the solar wind velocity is assumed to be purely radial, then its dependence on the radial magnetic field component seems strange, because in the case of parallel velocity and magnetic field, the magnetic field does not act on the plasma.

The point is that the solar wind acceleration begins at much smaller heights. The solar wind is blown out as if from a nozzle or a chimney. Although the field is radial directly on the source surface, its strength is determined by the entire field structure in a spherical layer from the photosphere to the source surface. The correlation between the field strength on the source surface and the radial plasma outflow arises precisely in this way.

EVOLUTION OF THE COMPONENT OF SOLAR WIND FLOWS FROM STREAMERS DURING SOLAR CYCLE 23

An interesting feature is revealed for one type of flows associated with streamers.

The dependence of R_{in} on $|B|$ for streamers can be expressed as

$$R_{in} = R_0 \times |B_R|^{-\alpha}, \qquad (2)$$

which is a straight line in a log–log coordinate system.

The meaning of the characteristics in Eq. (2) is the following. The quantity R_0 corresponds to an arbitrary location of the transition region boundary in the case of $|B| \approx 1$ μT. The parameter α specifies the degree of correlation between the field and the flow speed, because $R_{in} \sim v^{-1}$. In general, the distance to the "sonic point" depends not only on the speed of the solar wind but also on its temperature and magnetic field. In the case under consideration, we simply relied on experimental works. The existence of an inverse relationship between the location of the inner boundary of the transonic region and the solar wind speed $R_{in} \sim v^{-1}$ was established by Lotova et al. (1992, 2002). In the first paper, this relationship was found from radio-astronomical experiments; in the second paper, spacecraft data on the solar wind speed were invoked. Other relationships implicitly enter into the general dependence of the distance to the sonic point on velocity.

In the subsequent study of the formation of the supersonic solar wind flow, we should take into account the fact that Figs. 1 and 2 were obtained from the experimentally studied radial dependences of radio wave scattering characteristics: the scattering angle $2\Theta(R)$ and the scintillation index $m(R)$. The structural features of the radial profiles $2\Theta(R)$ and $m(R)$ coinciding in these characteristics allow the position of the solar wind critical point R_{in} to be determine on the scale of radial distances from the Sun. The set of data on the spatial position of the solar wind sonic point R_{in} obtained in this way was used in Figs. 1 and 2. The other parameter B_R used in Figs. 1 and 2, the magnetic field strength in the solar corona at point R conjugate to the position of the critical point R_{in}, was calculated by the method described by Obridko et al. (2012), Obridko and Yermakov (1989), and Obridko and Schelting (1992).

R_{in} decreases with increasing α at a fixed field strength, implying an increase in the flow speed.

This relationship exhibits an interesting variation with time. In the rising phase of the cycle (Fig. 1), a rather strict linear dependence is established:

$$\log R_{in} = \log R_0 - \alpha \log |B_R|. \qquad (3)$$

The exponent of the power-law dependence α changes little, slightly decreasing to the cycle maximum, but from year by year the ranges of $\log R_0$ and $\log |B_R|$ increase. Within each year, the decreasing dependence of $\log R_{in}$ on $\log |B_R|$ is retained, i.e., the solar wind speed increases with $|B_R|$ on short time scales.

This implies that the solar wind acceleration mechanism changes its parameters only slightly during this entire period in the rising phase of cycle 23. At the same time, however, the effective characteristic

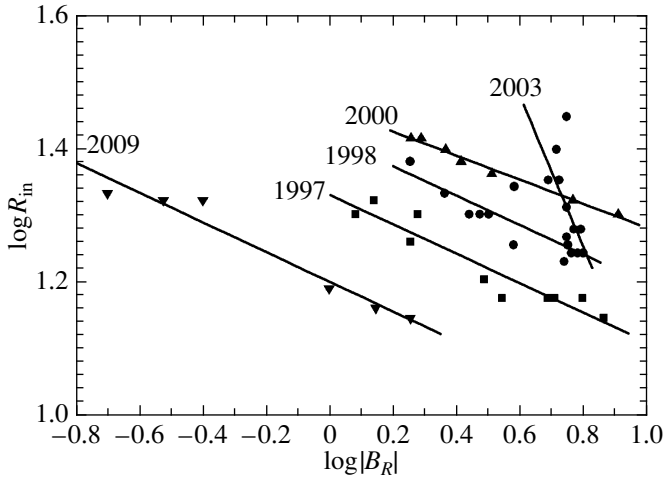

Fig. 1. Dependence of log R_{in} on magnetic field strength log $|B_R|$ in the rising phase of cycle 23.

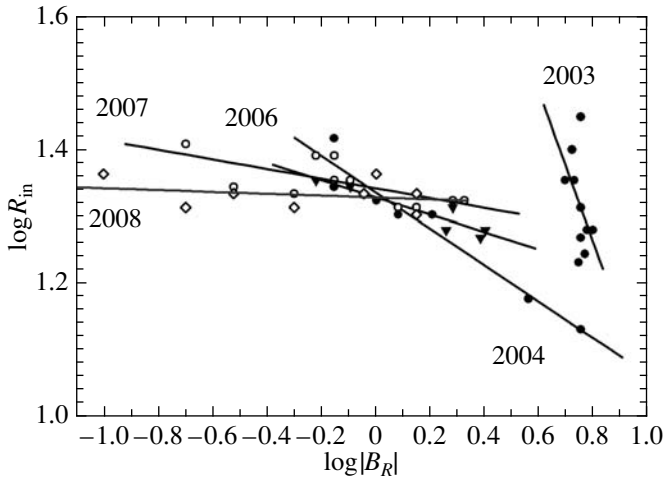

Fig. 2. Dependence of log R_{in} on magnetic field strength log $|B_R|$ in the declining phase of cycle 23.

sizes of the acceleration region decrease due to a strengthening of the local fields. This causes the effective value of R_0 to increase, i.e., again suggests an increase in the flow speed.

This continued until 2003, in which the values of $|B_R|$ lie in such a narrow range that the linear approximation becomes meaningless. After 2003 the situation changed dramatically (Fig. 2). Now, at the mean values of R_{in} and $|B_R|$ changing relatively little, the slope α changes, approaching almost zero at the cycle minimum.

This probably implies that the main solar wind acceleration mechanism changed in 2003. After reaching a significant maximum in 2003–2004, α decreased rapidly and the distance R_{in} virtually ceased to depend on the magnetic field. This implies a transition to the classical nonmagnetic expansion of the solar corona.

INTERPRETATION OF EXPERIMENTAL DATA

The experimentally observed changes of the characteristics in dependence (2) are probably related to different effects of magnetic fields with different scales on the solar wind speed. It should be kept in mind that the contribution from these fields varies with cycle phase. The thin line in Fig. 3 indicates the traditional sunspot numbers (R_z). The thick line indicates the

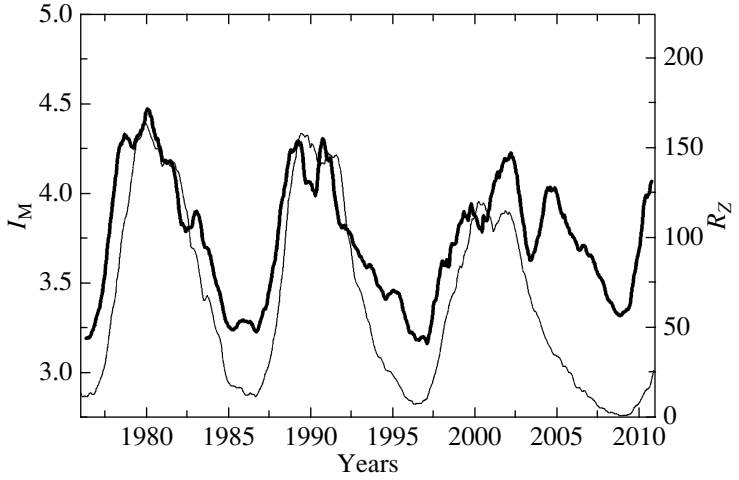

Fig. 3. Time dependence of the effective multipole index I_M (thick line) and sunspot number R_Z (thin line).

effective multipole index I_M used by Obridko et al. (2012),

$$I_M = -0.5\log(I_s/I_\odot)/\log(2.5),$$

where I_s and $I_\odot$ are the mean values of the square of the radial magnetic field component at the levels of the source surface ($r = 2.5R_\odot$) and the photosphere ($r = R_\odot$), respectively.

The index I_M defines the contribution from large-scale and small-scale fields. The index I_M approaches a dipole value of 3 when global fields with length scales comparable to the solar radius dominate on the Sun and 5 when smaller scale fields dominate at the cycle maxima.

It can be seen from Fig. 3 that after the maximum of cycle 23 in 2000–2001, I_M decreased sharply and reached almost the dipole value by 2003. In general, such a decrease was also observed in cycle 22, but it was much smaller and closer to the cycle maximum at that time.

For the subsequent analysis, it is important that I_M reflects precisely the energy contribution from fields of different scales; it is insensitive to structural changes of the fields. Therefore, it takes on a quasi-dipole value both at the minimum, when the axial dipole dominates, and in the declining phase, when the equatorial dipole often dominates (Livshits and Obridko 2006). It is the equatorial dipole responsible for the low-latitude coronal holes and the heliospheric current sheet that determines the slow solar wind in the declining phase of the solar cycle. In this case, by the heliospheric current sheet we mean the magnetic equator separating the oppositely directed open magnetic fields on the Sun. This equator is curved and its shape is often compared with a ballerina skirt.

Here, we do not consider the interaction of the solar wind with the interplanetary medium.

In Fig. 4 the circles connected by the thin line indicate the solar wind speed near the Earth averaged over 27-day periods based on OMNI-2 data (ftp://nssdcftp.gsfc.nasa.gov/data/omni/). The black thick line indicates the magnetic moment of the equatorial dipole M_{eq} based on data from the John Wilcox Observatory (http://wso.stanford.edu/gifs/Dipall.gif). We see that the spike in speed in 2003 coincides with the increase in the magnetic moment of the equatorial dipole.

Note, however, that the cyclic variations of the equatorial dipole consist not only in the change of its amplitude but also in the rotation of the entire structure of the large-scale magnetic field and the increase in the tilt of the heliospheric current sheet.

During the cycle, the opening of the current sheet changes gradually. The half-sum of the limiting deviations of the neutral line from the equator is called the tilt and characterizes the gradual change in field scale on the source surface. It is this change that leads to an expansion of the bases of streamers and an increase of the latitude zone they occupy.

In Fig. 5 the black circles connected by the thick line indicate the change in $\log R_0$ and the black thin lines indicate the change in tilt Δ (http://wso.stanford.edu/gifs/Tilts.gif). It is commonly assumed that when the tilt Δ reaches 70°, the polar field reversal phase begins. This phase lasts 1–1.5 years and roughly corresponds in time to the phase of the solar activity maximum.

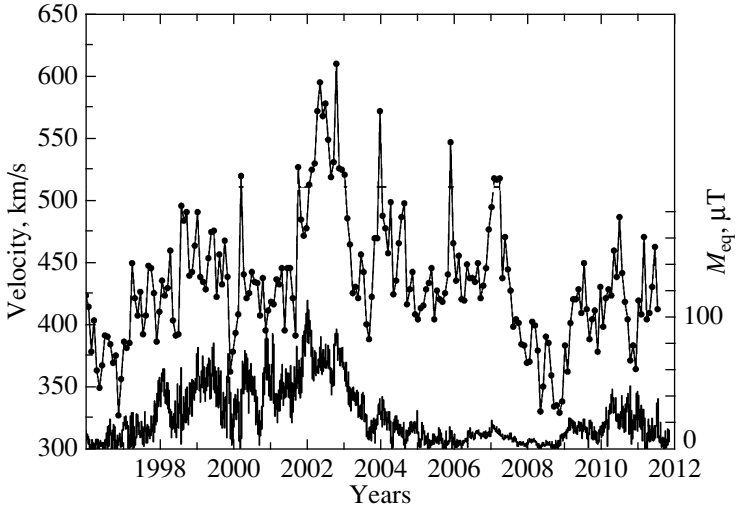

Fig. 4. Time dependences of the solar wind speed (circles and thin line) and the magnetic moment of the equatorial dipole (thick line).

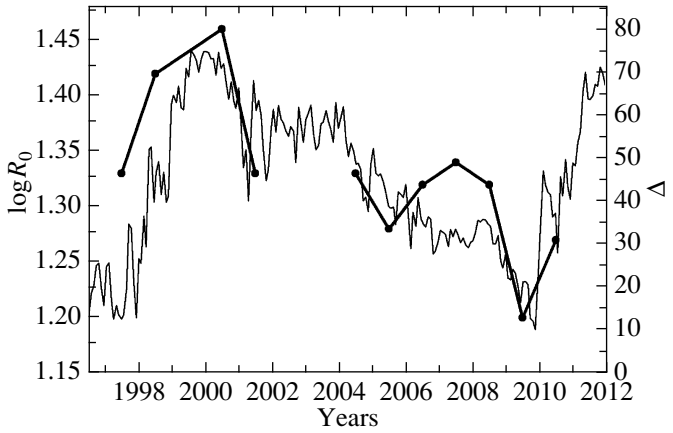

Fig. 5. Time dependences of $\log R_0$ (circles and thick line) and the opening of the heliospheric current sheet Δ (thin line).

In Fig. 6 the circles and the thin line indicate the change in α, the exponent of the exponential dependence $R_{in}(|B_R|)$; the thick line indicates the change in the amplitude of the equatorial dipole M_{eq} (http://wso.stanford.edu/gifs/DipallR.gif). The values of α for 2003 were excluded as unreliable (see Figs. 1 and 2).

We see that there is a certain similarity in the behavior of the curves $\log R_0$ and Δ. Note that the sharp rise in the amplitude of the equatorial dipole led to a dramatic increase in α. Subsequently, both quantities fell synchronously, simultaneously reaching the minimum. Significantly, α in 2009 virtually coincides with α in 1997, while in 2010 it is close to α at the maximum of cycle 23 in 2000. The point is that the rising phase of cycle 24 was very short and the equatorial dipole reached its maximum already in 2010. This suggests a certain similarity in the correlation between α and M_{eq} in two neighboring cycles, despite the difference in power between these cycles.

Thus, the cyclic variation of the dependence $R_{in}(|B_R|)$ seems to be the result of a complex interaction between fields of different scales. In the rising phase of solar activity, the contribution from local fields leads to an increase in the opening of the heliospheric sheet and the amplitude of the equatorial dipole, which is reflected in a gradual shift of the range of R_{in} and $|B_R|$ to higher values. The sizes of the streamer bases also grow. At the same time, within

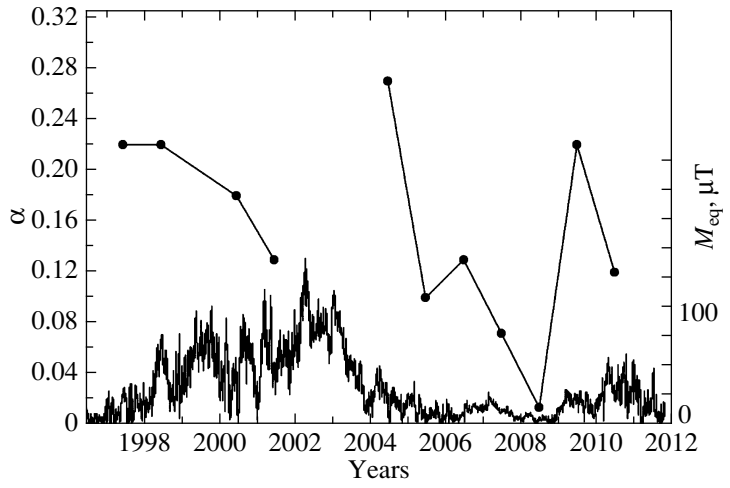

Fig. 6. Time dependences of the exponent of the exponential dependence α (circles and thin line) and the magnetic moment of the equatorial dipole M_{eq} (thin line).

each year the negative correlation between R_{in} and $|B_R|$ is retained. Thus, the solar wind acceleration has a magnetic character in this period. As was shown by Lotova et al. (1992, 2002), the smaller the R_{in}, the larger the corresponding solar wind speed. Thus, the negative correlation between R_{in} and $|B_R|$ points to the positive correlation between the speed and magnetic field observed at that time. Previously, a positive correlation between the magnetic field and the brightness of the green corona was found by Badalyan and Obridko (2006, 2007). In turn, this correlation was interpreted by Badalyan and Obridko as a consequence of a nonwave coronal heating mechanism. This correlation is especially significant two years after the cycle maximum, when the equatorial dipole reached its maximum. At that time, the local fields still retained their high values, but strong large-scale fields joined them.

After 2003 the local fields decayed and the contribution from large-scale fields increased with the simultaneous dipole rotation to the axial position. Both the solar activity and global field characteristics (R_Z and M_{eq}) and the main characteristic of the correlation between the distance to the sonic point and the magnetic field α began to decrease synchronously. The decrease in the speed–field correlation probably stems from the fact that the wave sources of coronal heating, which are characterized by a weak (or even negative) correlation between the field and corona brightness, increase in importance at this stage (Badalyan and Obridko 2006, 2007).

Generally, the position of the sonic point is determined not only by the heating rate but also by the configuration of the streamlines (in other words, by the fact that the flow is not one-dimensional). However, we could not take into account such subtle effects and the structure was assumed to be homogeneous within a fairly wide flow.

Of course, this work does not purport to attempt to figure out the coronal heating mechanism. Many other works, including our papers, are devoted to the coronal heating mechanisms. We pay attention to a new interesting feature of the correlation between the magnetic field in the solar corona and the solar wind speed. This feature coincides with the sharp restructuring of the magnetic field on the Sun.

As is well known, all coronal heating mechanisms break up into two classes. Some of the models (DC) are based on slow magnetic field dissipation, other models (wave models, AC) rely on the dissipation of Alfvén waves of various types. For an overview of the models, see Aschwanden (2004) and Mandrini et al. (2000). It turned out that both mechanisms are involved in heating, but their relative role depends on the contribution from fields of different scales (Badalyan and Obridko 2006, 2007).

Thus, our analysis of the correlation between the solar wind speed and the magnetic field in the solar corona confirms the hypothesis about the dual character of the coronal heating mechanisms. In the rising phase and at the cycle maximum, the coronal heating mechanisms related to the magnetic field (DC), which are probably determined by microflares and reconnection, are more efficient.

In the declining phase of the solar cycle, the dependence on the magnetic field drops. At this stage wave heating (AC) is more efficient.

ACKNOWLEDGMENT

This work was supported by the Russian Foundation for Basic Research (project no. 11-02-00259a).

REFERENCES

1. M. J. Aschwanden, *Physics of the Solar Corona: An Introduction* (Springer, Berlin, 2004).
2. O. G. Badalyan and V. N. Obridko, Solar Phys. **238**, 271 (2006).
3. O. G. Badalyan and V. N. Obridko, Astron. Lett. **33**, 182 (2007).
4. M. Kodjima, K. Asai, K. Hakamada, T. Ohmi, et al., ATP Conf. Prog. **471**, 29 (1998).
5. I. M. Livshits and V. N. Obridko, Astron. Rep. **50**, 926 (2006).
6. N. A. Lotova, O. A. Korelov, and E. V. Pisarenko, Geomagn. Aeron. **32**, 78 (1992).
7. N. A. Lotova, K. V. Vladimirskii, V. N. Obridko, et al., Solar Phys. **205**, 149 (2002)
8. N. A. Lotova, K. V. Vladimirskii, and V. N. Obridko, Geomagn. Aeron. **50**, 711 (2010).
9. N. A. Lotova, K. V. Vladimirskii, and V. N. Obridko, Solar Phys. **269**, 129 (2011).
10. C. H. Mandrini, J. Der Moulin, and A. Klimchuk, Astrophys. J. **530**, 999 (2000).
11. V. N. Obridko and F. A. Yermakov, Astron. Tsirk. **1539**, 24 (1989).
12. V. N. Obridko and B. D. Schelting, Solar Phys. **173**, 167 (1992).
13. V. N. Obridko, E. V. Ivanov, A. Ozguc, et al., Solar Phys. **281**, 779 (2012).
14. R. Schwenn, Space Sci. Rev. **124**, 51 (2006).

Translated by G. Rudnitskii